Journal of Nuclear Materials 61 (1976) 192–202
© North-Holland Publishing Company

OXYGEN REDISTRIBUTION IN FAST REACTOR OXIDE FUEL

C. SARI
Commission of the European Communities, European Institute for Transuranium Elements, Karlsruhe, Germany

G. SCHUMACHER
Institut für Neutronenphysik und Reaktortechnik, Kernforschungszentrum Karlsruhe, Germany

Received 1 February 1976

Out-of-pile tests were carried out in order to investigate the oxygen redistribution in uranium-plutonium mixed oxides exposed to a thermal gradient. In hypostoichiometric oxide fuel the oxygen migrates towards the low temperature region of the pellet and in hyperstoichiometric fuel the oxygen migrates in the opposite direction. The oxygen transport is explained on the basis of solid-state thermal diffusion and occurs via vacancies and interstitials. It has been shown that the heats of oxygen transport are a function of plutonium and uranium valencies for hypo- and hyperstoichiometric oxides, respectively. The experimental results allowed to construct a practical example in which oxygen profiles in fuel pins were calculated as a function of initial stoichiometry and burnup.

Des essais hors-pile ont été entrepris afin d'étudier la redistribution de l'oxygène dans des oxydes mixtes d'uranium et de plutonium exposés dans des gradients de température. Dans le combustible d'oxyde sous-stoechiométrique l'oxygène migre vers la région de basse température de la pastille de combustible cependant que dans l'oxyde sur-stoechiométrique l'oxygène migre dans la direction opposée. Le transport d'oxygène est expliqué sur la base de la diffusion thermique dans l'état solide par l'intermédiaire des lacunes et des interstitiels. Il a été montré que les chaleurs de transport de l'oxygène sont fonction des valences du plutonium et de l'uranium respectivement pour les oxydes sous- et sur-stoechiométrique. Les résultats expérimentaux permettent de construire un modèle pratique dans lequel les profils de concentration en oxygène dans les aiguilles du combustible sont calculés en fonction de la valeur du rapport initial O/M et du taux de combustion.

Es wurden Laborversuche zur Untersuchung der Sauerstoffumverteilung in Uran-Plutonium-Mischoxiden unter Einfluss eines Temperaturgradienten durchgeführt. Der Sauerstoff wandert in unterstöchiometrischem Oxidbrennstoff zu den Brennstoffzonen mit niedrigen Temperaturen und in überstöchiometrischem Brennstoff in die umgekehrte Richtung. Der Sauerstofftransport geschieht durch Thermodiffusion in der festen Phase über Leerstellen und Zwischengitterplätze. Es wird gezeigt, dass die Überführungswärmen für den Sauerstofftransport im unter- bzw. überstöchiometrischen Zustand von der Wertigkeit des Plutoniums bzw. des Urans abhängen. In einem praktischen Beispiel werden anhand der experimentellen Ergebnisse Sauerstoffprofile in Mischoxidbrennstäben als Funktion des anfänglichen O/M-Verhältnisses und des Abbrandes berechnet.

1. Introduction

During the last years, theoretical and experimental works have shown that a marked redistribution of oxygen occurs in reactor oxide fuel pins. Rand and Roberts [1] first described the transport of oxygen via the gas phase in uranium-plutonium mixed oxides. They proposed a transport mechanism involving CO/CO_2 and H_2/H_2O gas mixtures existing in the pores and cracks of the fuel. A quantitative prediction of this phenomenon was given by Rand and Markin [2] who indicated that oxygen migrates to lower temperatures in hypostoichiometric oxides whereas it migrates to higher temperatures in hyperstoichiometric oxides.

The first experiments on oxygen redistribution in hypostoichiometric mixed oxide fuels carried out by Evans et al. [3] confirmed that oxygen was transported to the fuel regions with lower temperatures. In these experiments solid state thermal diffusion and gas

phase transport of oxygen via the carrier gases H_2O and CO_2 could take place simultaneously in the solid matrix and in the gap surrounding the mixed oxide pellets. To describe this process which operates via several alternative oxygen transport paths, Aitken [4] developed a cyclic flow model of thermotransport. This treatment is particularly applicable to materials with cracks and channels of interconnected porosity, i.e. the unrestructured fuel region. In the dense fuel region the cracks produced by thermal shocks were filled in a relatively short time by condensation of fuel material. Thus, in this region only solid state thermal diffusion determines the steady state distribution of oxygen.

First experiments on oxygen redistribution by solid state thermal diffusion in which gas phase transport was negligible were carried out by Bober et al. [5]. These experiments revealed that in hypostoichiometric mixed oxides, oxygen migrates to lower temperatures, but the local O/M ratio does not exceed 2.00.

Later investigations showed that the heat of transport of the processes described above depends on the stoichiometry of the fuel both in experiments with combined solid state and gas phase transport [3,6] and with solid state transport alone [7,8]. One of the combined experiments [3] revealed, moreover, the effective heat of transport to be dependent on the concentration of plutonia at constant oxygen activity, i.e., at constant O/Pu ratio [3]. In solid state thermal diffusion, on the contrary, the heat of transport should be only a function of the differences in the oxygen activity, as revealed by a comparison of oxygen transport in uranium-plutonium mixed oxides and in plutonium oxides [8].

In this work solid state oxygen transport in hypo- and hyperstoichiometric oxide fuels has been investigated as a function of O/M and U/Pu ratios. The aim is to obtain data for calculation of oxygen profiles in reactor fuel.

2. Experimental

Cylindrical pellets of coprecipitated uranium-plutonium mixed oxide with densities between 94 and 96% of the theoretical density were used. To minimize the gas exchange along the temperature gradient, the hypostoichiometric pellets destined for the axial experiments were coated with metallic molybdenum. Two experimental methods were used to investigate the redistribution of oxygen caused by thermal diffusion. One uses an axial, the other a radial temperature gradient across the fuel pellet.

The experiments with the radial temperature gradient were conducted by heating the pellet with an alternating current flowing in axial direction. The pellets were placed between two tungsten electrodes during the experiment. The temperature at the pellet periphery was established by free heat radiation and was measured with an optical pyrometer, whilst the central temperature was computed. Details of the apparatus have been published elsewhere [9].

The experiments with the axial temperature gradient were carried out with an induction heated equipment described previously [5]. Briefly, the general arrangement was a pellet encapsulated in a cylindrical tungsten or molybdenum container which was induction heated at one end and cooled at the other end. The mixed oxide pellets were closely fitted in the container to hinder the transport via the gas phase. Temperatures were measured at the high and low temperature side of the container with an optical pyrometer and a thermocouple, respectively.

For the determination of the redistribution effects, samples were taken from both the high and low temperature sides of each pellet. Their O/M ratio was determined by measuring the weight change after equilibration with CO/CO_2 at 850°C and by *X*-ray diffraction. The uncertainties are in the range of ±0.003.

3. Theoretical

For treating the thermal diffusion of oxygen one needs only to deal with the oxygen sublattice of the mixed oxide because the diffusion coefficient of oxygen is several orders of magnitude higher than that of uranium and plutonium. This is due to the fluorite structure of the mixed oxide, characterized by a perfect cation lattice and anionic vacancies and interstitials. A distinction is made between the hypostoichiometric and the hyperstoichiometric systems. The first can be considered to be a pseudobinary system, consisting of a dilute solution of oxygen vacancies in the oxygen sublattice; the second can be described as a dilute solution of interstitial oxygen atoms.

The deviation from stoichiometry in a mixed oxide having the composition of $(U, Pu)O_{2+y}$ is given by:

$$y = \frac{O}{U + Pu} - 2 , \tag{1}$$

which is related to a single molecule of mixed oxide.

In the hypostoichiometric state y is negative and represents the number of vacancies per oxide molecule; i.e. in the oxygen sublattice the atomic fraction of vacancies x_v is:

$$x_v = -y/2 . \tag{2}$$

In the hyperstoichiometric state y represents the number of interstitial oxygen atoms per oxide molecule, and the atomic fraction of the interstitial atoms x_i becomes:

$$x_i = y . \tag{3}$$

With the definitions given in eqs. (2) and (3), thermal diffusion of oxygen vacancies and interstitials in the hypo- and hyperstoichiometric mixed oxides, respectively, can be described using flux equations derived from the thermodynamics of irreversible processes [10–12]. The flux of oxygen vacancies, J_v, in the oxygen sublattice of hypostoichiometric mixed oxide is:

$$J_v = -ND_v \left[\nabla x_v + \frac{(1 - x_v)x_v}{1 + (\partial \ln \gamma_v / \partial \ln x_v)} \frac{Q_v^*}{RT^2} \nabla T \right] , \tag{4}$$

whereas the flux of interstitial oxygen atoms in the hyperstoichiometric oxide becomes:

$$J_i = -ND_i \left[\nabla x_i + \frac{x_i}{1 + (\partial \ln \gamma_i / \partial \ln x_i)} \frac{Q_i^*}{RT^2} \nabla T \right] , \tag{5}$$

where N is the total number of oxygen atoms per unit volume, D_v, D_i the diffusion coefficients of vacancies and interstitial atoms, respectively, in the oxygen sublattice. γ is the activity coefficient, Q_v^*, Q_i^* the molar effective heats of transport of vacancies and interstitial atoms in the oxygen sublattice, respectively, R the gas constant and T the absolute temperature.

Applying the equation of continuity:

$$\operatorname{div} J + \frac{\partial x}{\partial t} = 0 \tag{6}$$

together with eqs. (4) and (5), it is now possible to calculate numerically the concentration profile of oxygen vacancies and interstitials, respectively, at a given time t by following a definite sequence of small time increments.

The oxygen mobility is high enough to ensure that a steady-state distribution of oxygen will be reached, i.e. the fluxes J_v and J_i, respectively, disappear. If into eqs. (4) or (5) the deviation from the stoichiometric state, y, is introduced as given by eqs. (2) and (3), respectively, the Soret coefficients are obtained, which describe the steady-state concentration gradient. Thus for the hypostoichiometric case:

$$\frac{1}{y} \frac{\nabla y}{\nabla T} = \frac{1 - (y/2)}{1 + 2(\partial \ln \gamma / \partial \ln y)} \frac{Q_v^*}{RT^2} \tag{7}$$

and for the hyperstoichiometric case:

$$\frac{1}{y} \frac{\nabla y}{\nabla T} = \frac{1}{1 + (\partial \ln \gamma / \partial \ln y)} \frac{Q_i^*}{RT^2} . \tag{8}$$

It should be noted that, by definition, the value of y must have a negative sign in eq. (7). In the case of dilute solutions the factors containing y on the right-hand side of eqs. (7) and (8) become unity.

Integration of eqs. (7) and (8) for dilute solutions with a constant value of Q^* gives for the steady state in hypo- and hyperstoichiometric material:

$$\ln y_2/y_1 = \frac{Q^*}{R} \left(\frac{1}{T_2} - \frac{1}{T_1} \right) . \tag{9}$$

The dependence of Q^* (either Q_v^* or Q_i^*) on y is considered during the numerical calculation of oxygen distribution.

In oxide fuels, which consist of ionic crystals, the ion fluxes are influenced by electric forces caused by the thermoelectric potential, ϕ, which appears in the temperature gradient; therefore, the heats of transport are quantities which include an electric term [12]:

$$Q^* = Q_g^* + \frac{ZT \cdot \nabla \phi}{\nabla T} . \tag{10}$$

Q_g^* is the share of the heat of transport caused by the lattice energies, Z the electric charge transported by the number of oxygen vacancies or interstitials that corresponds to the transport of one mole of oxygen in the opposite direction.

4. Results

All nonstoichiometric oxide pellets show marked differences in the O/M ratios between the high and low temperature side. In hypostoichiometric pellets the oxygen migrated down the temperature gradient whilst in hyperstoichiometric oxides it migrated in the opposite direction.

Eq. (9) is used for the calculation of the heats of transport, Q_v^* and Q_i^*, since it can be assumed that in our experiments a steady state oxygen distribution was attained. This assumption is supported by experi-

Table 1
Data from experiments with an axial temperature gradient in hypostoichiometric mixed oxide

Exp. no.	T_{max} (K)	T_{min} (K)	O/M_{HT}	O/M_{LT}	Time (h)	x_{Pu}	Length (mm)	$-Q_v^*$ (kcal/mol)
1	2320	1470	1.945	1.97	97	0.15	4	6.2
2	2250	1640	1.97	1.99	68	0.15	4	15.6
3	2370	1420	1.95	1.97	3	0.15	7.7	4.8
4	2370	1420	1.95	1.96	3	0.15	8.5	2.2
5	2370	1720	1.93	1.99	67	0.15	7.4	24.2
6	2370	1720	1.947	1.944	3	0.15	7.6	0
12	2050	1240	1.937	1.986	64	0.15	4	10.6
14	2500	1600	1.99	2.0	16	0.15	8	23.3
15	2370	2090	1.966	1.979	22	0.15	4	18.2
16	2080	1840	1.955	1.967	20	0.2	6.1	10
17	1970	1570	1.923	1.938	6	0.4	5.7	4
18	2270	1900	1.90	1.923	84	0.4	5.5	7
19	1900	1520	1.923	1.956	84	0.4	5.5	10.3
20	2370	2070	1.90	1.902	20	0.4	2.3	0.8
21	2070	1820	1.902	1.912	20	0.4	2.3	3.3
22	2370	1370	1.91	1.99	20	0.5	4.3	14.8
23	2370	1570	1.77	1.85	20	0.85	3.4	4.2
24	2020	1670	1.69	1.71	3	1.0	4.0	1.6
25	1670	1270	1.71	1.75	3	1.0	4.0	1.2

Table 2
Data from experiments with a radial temperature gradient in hypostoichiometric mixed oxide

Exp no.	T_{max} (K)	T_{min} (K)	O/M_{HT}	O/M_{LT}	Time (h)	x_{Pu}	Diam. (mm)	$-Q_v^*$ (kcal/mol)
7	2070	1670	1.98	1.99	1	0.15	5.6	14.6
8	2970	1970	1.982	2.0	0.1	0.15	5.7	30.6
9	2070	1670	1.978	1.986	6	0.15	5.67	29.8
10	2970	1970	1.988	1.996	0.25	0.15	5.9	15.2
11	1870	1570	1.958	1.979	5	0.15	5.65	16.6
13	2070	1670	1.98	1.99	3	0.15	5.6	14.6
26	2620	2300	1.79	1.90	0.3	1.0	4.5	26.6
27	2300	1920	1.90	1.97	0.3	1.0	4.5	25.5
28	2620	2140	1.79	1.90	0.3	1.0	4.8	16.8
29	2140	1920	1.90	1.95	0.3	1.0	4.8	25
30	2600	2300	1.85	1.90	0.3	1.0	4.5	15
31	2620	1920	1.75	1.90	1	1.0	4.2	10.5
32	2610	1920	1.78	1.90	0.3	1.0	4.6	11.2

ments which showed a high oxygen mobility at relatively low temperatures in uranium-cerium mixed oxide containing 20 mol.% cerium oxide. It was observed that the oxygen concentration in hypostoichiometric $(U_{0.8}Ce_{0.2})O_{2+y}$ specimens of high density equilibrates within 12 hours at 1060°C. One can anticipate the mobility in hypostoichiometric uranium-plutonium mixed oxide to be of the same order of magnitude [9]. This is confirmed by experiments with $(U_{0.85}Pu_{0.15})O_{2+y}$ with $y < 0$ in which the stoichiometric state with a CO/CO_2 atmosphere at 850°C has been attained after 12 h. Other experiments with stoichiometric mixed oxides in flowing pure hydrogen show a equilibration of the mixed oxide at 1480°C after less than 5 h. It is to be noted that the hydrogen flow through the thermobalance was only 3 ℓ per h. Chereau and Wadier [14] observed in PuO_2 a reduction to O/Pu = 1.975 with CO in about 30 min at 1080°C. They calculated a diffusion coefficient of some 10^{-4} cm/sec.

4.1. Hypostoichiometric fuel

The experimental conditions and results of the experiments with the axial and radial temperature gradients are presented in tables 1 and 2. Columns 2 and 3 contain the maximum and minimum temperatures of the specimens, respectively, whilst column 4 shows the quantities O/M_{HT} and O/M_{LT} which are the O/M ratios at the high and low temperature sides of the pellets, respectively.

For the evaluation one has to take into account that the samples for the O/M analysis have a thickness of 0.8 mm in the axial and 0.3 mm in the radial experiments, thus the given values are the averages of those in the fuel regions from which the samples were taken. The other columns contain the duration t of the experiments, the plutonium concentration x_{Pu}, the diameter d and length l of the specimens. The tables show also the respective heats of transport Q_V^* of oxygen vacancies calculated from eq. (7) under the assumption of a steady state oxygen distribution at the end of the experiment.

The heats of transport of oxygen vacancies given in table 1 are depicted in fig. 1 as a function of plutonium valence V_{Pu}. Though the scatter of the values is rather high the plot indicates that for low O/M ratios near the trivalent state of plutonium Q_V^* vanishes. The scatter increases with increasing O/M ratios due to the higher influence of the error in the O/M analysis in the vicinity of the stoichiometric state. Fig. 1 also illustrates the approximate dependence of Q_V^* on V_{Pu}. The function can be fitted by the following equation:

$$Q_V^* = -9.45 \times 10^5 + 5.66 \times 10^5 V_{Pu} - 8.5 \times 10^4 V_{Pu}^2, \quad (11)$$

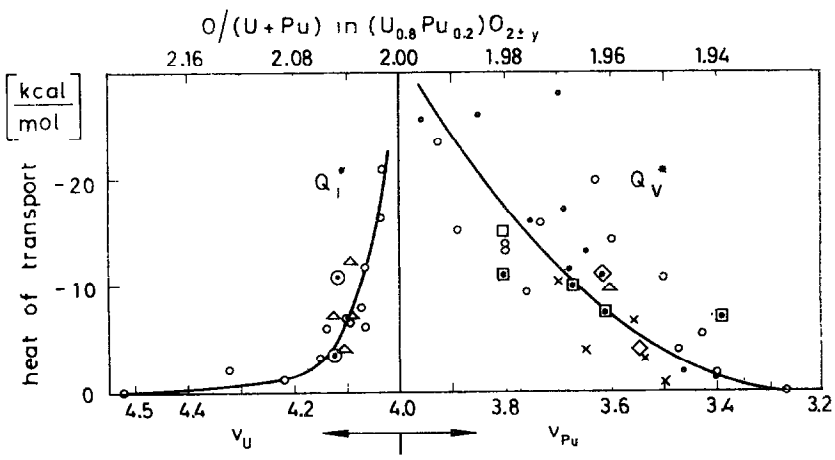

Fig. 1. Measured heat of transport of oxygen vacancies (right) and of oxygen interstitials (left) in hypo- and hyperstoichiometric mixed oxides respectively. Abscissa: plutonium valency V_{Pu} and uranium valency V_U (below) and O/(U + Pu) ratio (above). Values of this work: ○ 15, △ 20, + 30, × 40, □ 50, ◇ 85, · 100 mol% plutonium oxide. Values of other authors: ⊙ [10], ⊡ [3], 15 mol% and ◈ [6], 25 mol% plutonium oxide.

which fits the whole values better than the linear function given for Q_v^* in a former representation [7].

Values of Q_v^* for pellets with high plutonium concentrations and of pure plutonium oxides are also plotted in fig. 1. These values do not differ markedly from those obtained for pellets with Pu/(U + Pu) = 0.15. Thus beyond the error limits no dependence of Q_v^* on the plutonium content was observed.

4.2. Hyperstoichiometric fuel

The hyperstoichiometric pellets were treated in a radial temperature gradient. The conditions and results of these experiments are given in table 3 which is arranged similar to tables 1 and 2. The samples used for the O/M analysis had a thickness of 0.3 mm.

The heat of transport of oxygen interstitial atoms Q_i^* was calculated using eq. (9) and assuming a steady state oxygen redistribution at the end of each heat-treatment. The values of Q_i^* are represented in fig. 1 as a function of uranium valence V_U. The values fit rather well the depicted line in fig. 1 which can be expressed by

$$Q_i^* = -8.3 \times 10^{33} \exp(-17\, V_U)\,. \tag{12}$$

The scatter of values is lower than for the hypostoichiometric material. The experiments with oxides of different plutonium content indicate that the value of Q_i^* is not marked influenced by the plutonium concentration.

5. Discussion of the results

The experimental results show that the solid state heat of transport depends on the plutonium and uranium valence but not on the plutonium concentration.

5.1. Hypostoichiometric fuel

In hypostoichiometric uranium-plutonium mixed oxide fuel the heat of transport of oxygen vacancies diminishes with decreasing plutonium valence and approaches zero at a valence of about 3.3.

Table 3
Data from experiments with a radial temperature gradient in hyperstoichiometric mixed oxide

Exp no.	T_{max} (K)	T_{min} (K)	O/M_{HT}	O/M_{LT}	Time (h)	x_{Pu}	Diam. (mm)	$-Q_i^*$ (kcal/mol)
1	2470	2170	2.04	2.016	5	0.15	5.95	6.7
2	2270	1470	2.09	2.08	3	0.15	6.0	1.0
3	2870	1670	2.08	2.05	1.5	0.15	5.9	8.0
4	2655	2390	2.06	2.03	1.5	0.15	5.95	7.5
5	2600	2400	2.05	2.03	3	0.15	5.95	6.8
6	2770	1870	2.04	2.02	0.8	0.15	6.0	8.0
7	2770	1870	2.1	2.09	1	0.15	6.0	1.2
8	2570	1870	2.04	2.016	1	0.15	5.9	11.5
9	2770	1870	2.15	2.12	1	0.15	6.0	2.4
10	2770	1870	2.075	2.045	2	0.15	5.8	5.9
11	2770	1870	2.025	2.006	2	0.15	5.9	16.5
12	2440	1820	2.05	2.03	2.5	0.2	6.0	7.3
13	2390	1870	2.05	2.04	2	0.2	5.95	3.8
14	2410	1890	2.06	2.03	2	0.2	6.0	12
15	2370	1770	2.07	2.04	1	0.2	5.95	7.8
16	3070	1970	2.23	2.22	1	0.3	5.6	0.5
17	3020	1970	2.1	2.06	2	0.3	5.6	1.83
18	3020	1970	2.16	2.04	1	0.3	5.6	0.16
19	2070	1970	2.02	2.003	0.5	0.3	5.6	21
20	2070	1970	2.003	2.0001	1	0.3	5.6	37.5

The maximum value of Q_v^* is reached when the plutonium valence nears 4. In the range of plutonium valencies 3.4 to 3.8 the heats of transport are in accordance with those found by Evans et al. [3], as shown in fig. 1. However, their values were obtained from gas phase experiments allowing oxygen transport processes. Since gas transport was prevented in our experiments, this agreement indicates the solid state transport of oxygen to be the dominating process in hypostoichiometric fuels at least up to plutonium valencies of 3.8. A value of $Q_v^* = -11.7$ kcal/mol obtained by Aitken et al. [6] from a radial experiment is also in agreement. For valencies approaching the value of 4 no reliable determination of Q_v^* is possible since the error in the oxygen analysis is higher than the actual value of y. Moreover, the use of the logarithm in this range causes a very high scatter of Q_v^* values. Thus, the value of $Q_v^* = -102$ kcal/mol found by Evans et al. [3] is questionable since its associated scatter can be higher than one order of magnitude. Therefore, we do not report data in this region.

With respect to the values estimated in experiments allowing gas phase transport it is to be noted that transport quantities concerning the gas phase are not heats of transport per definition. The heat of transport is defined as the energy transferred by an activated jump process of an atom from one site to another [15].

At present the reason for the disappearance of Q_v^* at low O/M ratios cannot be given. One explanation could be an increase in the thermoelectric power with decreasing O/M ratios.

The results do not indicate whether Q_v^* is temperature dependent or not. Since the oxygen potentials at constant O/M ratios can be assumed to be approximately a linear function of temperature [2], one should not anticipate a temperature effect on Q_v^*. However, a marked temperature effect on Q_v^* could arise from the thermoelectric potential. But no facts are known of this phenomenon in hypostoichiometric mixed oxide fuels.

An interesting point is whether Q_v^* of these out-of-pile experiments and that of a reactor fuel pin will differ significantly. There is obviously no difference in the lattice energies at the high temperatures considered A difference could be caused by the tungsten and molybdenum containers, used in the axial experiments. However, the difference should not be large. This results from the comparison of Q_v^* values obtained from the radial and axial experiments. Thus one can assume that the thermoelectric potential of the mixed oxide and tungsten or molybdenum have the same signs and the same orders of magnitude. With respect to the irradiated fuel it should be noted that the reported Q^* values can be used for the determination of oxygen profiles, because Q^* depends on the uranium and plutonium valencies, which are estimated from the oxygen balance.

5.2. Hyperstoichiometric fuel

In hyperstoichiometric uranium-plutonium mixed oxide fuel the heat of transport of oxygen interstitials Q_i^* decreases with increasing uranium valence. It approaches to zero at a uranium valence of about 4.3 and attains a maximum value when the valence nears 4. As in hypostoichiometric oxides, the Q_i^* values in the region close to an uranium valence of 4 cannot be determined with reliability. Thus, our Q_i^* value of -37 kcal/mol and that found by Adamson and Carney [16] of about -50 kcal/mol for the near stoichiometric mixed oxide are doubtful, whilst for the uranium valence of 4.12 good agreement exists (fig. 1).

The negative sign of the heat of transport of the oxygen interstitials Q_i^* indicates that oxygen migrates up the temperature gradient. This is contrary to what is to be expected from a consideration of the forces of the lattice energies which lead to oxygen migration down the temperature gradient. This indicates that the thermoelectric forces are more effective than the lattice forces in hypostoichiometric mixed oxide fuels. Thermoelectric forces originate from the gradient of the thermoelectric potential which results from the thermal diffusion of electrons down the temperature gradient. This mechanism occurs at temperatures above 1200°C.

Markin et al. [1,2] and Adamson and Carney [16] explained oxygen migration up the temperature gradient in hyperstoichiometric fuel by the mechanism of gas phase transport. They assume that CO/CO_2 and H_2/H_2O mixtures are always present in fuel pins and can migrate by way of cracks and pores. However, since high density fuel pellets (94 to 96% th.d.) were used in our experiments gas phase transport did not play role in oxygen migration. In reactor fuel the restructuring produces rapid densification and healing of cracks, thus preventing effective radial gas transport.

6. Calculation of the oxygen redistribution in mixed oxide fuel pins

A knowledge of the Q_v^* and Q_i^* values allows the evaluation of the radial oxygen redistribution in reactor fuel pins. Calculations have been simplified by making the following assumptions. First a steady state oxygen redistribution occurs in a short time. Secondly, the Q^* values are independent of temperature, because in our experiments no marked dependence could be observed in the temperature range of 1200 to 2700°C. Thirdly, solid state transport is the predominant mechanism because oxygen is highly mobile in the solid phase of both, hypo- and hyperstoichiometric fuel and the gas transport paths via connected pores represent less than 5% of the total fuel. Even assuming an oxygen gas transport in the unrestructured zone, the oxygen profile does not significantly differ from those calculated on the basis of solid state transport. The results of comparative calculations are exemplified in fig. 2 for hypostoichiometric fuel.

During the numeric computation of the oxygen distribution with eq. (9) the Q^* values were varied as function of y in accordance with eqs. (11) and (12). A temperature profile [19] from a RAPSODIE monitor irradiation experiment was taken as typical. The temperature at the rim of the fuel was 1240 K and at the center 2600 K. Calculated oxygen profiles in fuel pins are illustrated in fig. 3, where the plutonium and uranium valencies are plotted against the relative radius. The parameter is the overall plutonium and uranium valence. Fig. 4 gives another representation of the diagram of fig. 3. It expresses the concentration of oxygen by the O/(U + Pu) ratio in $(U_{0.8}Pu_{0.2})_{2\pm y}$. Parameters at the lines are the overall O/(U + Pu) ratios. The diagrams describe the variation of the oxygen concentration as a function of the relative radius for the assumed overall valencies and O/(U + Pu) ratios. There result strong deviations from O/(U + Pu) = 2 of the oxygen concentrations in the interior and concentrations of approximately 2 at the rim of the fuel.

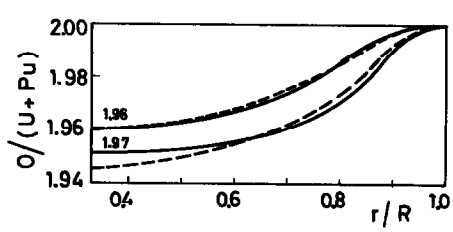

Fig. 2. Calculated radial oxygen distribution in $(U_{0.8}Pu_{0.2})O_{1.98}$ and $(U_{0.8}Pu_{0.2})O_{1.97}$ assuming solid state transport alone (solid lines) and a combined solid state gas-phase transport [3,4] in the outer fuel region with $r/r_0 > 0.8$ (dashed lines).

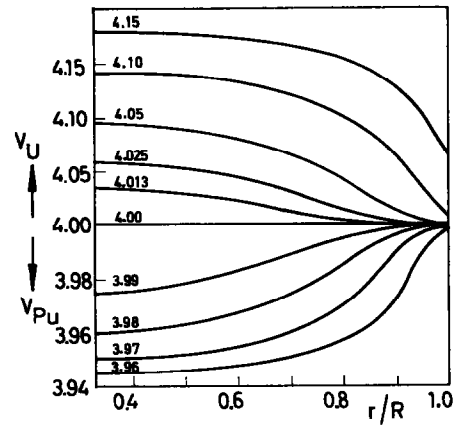

Fig. 3. Calculated radial oxygen distributions in (U, Pu)$O_{2\pm y}$ as a function of the uranium and plutonium valency V_U and V_{Pu} respectively. Parameters are the overall valencies.

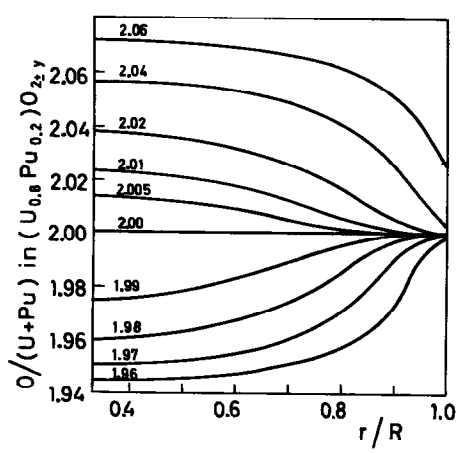

Fig. 4. Calculated radial oxygen distribution in $(U_{0.8}Pu_{0.2})O_{2\pm y}$ as a function of the O/(U + Pu) ratio. Parameter is the overall O/(U + Pu) ratio.

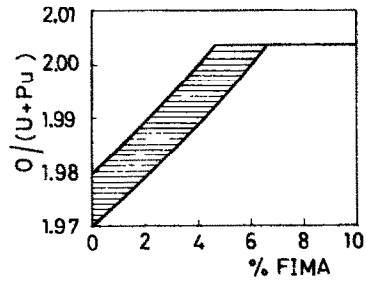

Fig. 5. Calculated increase of the overall O/(U + Pu) ratio as a function of burnup in a mixed oxide fuel, $(U_{0.8}Pu_{0.2})O_{2\pm y}$, with an initial O/(U + Pu) ratio between 1.97 and 1.98.

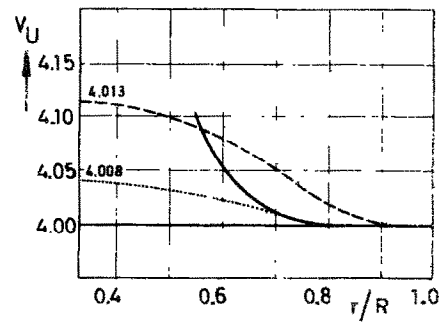

Fig. 6. Influence of fission-product molybdenum on the radial oxygen distribution in hyperstoichiometric mixed oxide. Dotted line: distribution when Mo is not fully oxidized Dashed line: distribution when Mo is fully oxidized. Full line. equilibrium (Mo – U, Pu) oxide.

During reactor operation the overall O/(U + Pu) ratio increases with burnup because oxygen is liberated by fission of uranium and plutonium. This process must be considered for the estimation of the change in the oxygen profile under irradiation. The increase of the O/(U + Pu) ratio with burnup is exemplified in fig. 5 for initial O/(U + Pu) ratios between 1.97 and 1.98. It has been calculated using an oxygen balance for mixed oxide fuel as a function of burnup [20]. The reaction of oxygen with the cladding material has not been taken into account.

In fig. 5 the overall O/(U + Pu) ratio increases continuously up to 2 by oxydation of the hypostoichiometric mixed oxide.

Above O/(U + Pu) = 2 the O/(U + Pu) ratio does not exceed the value at which the mixed oxide is in thermodynamic equilibrium with MoO_2. It results that at 9% burnup, 70% of the molybdenum is oxidized in the fuel with an initial O/(U + Pu) ratio of 1.98. The buffering function of molybdenum is enhanced by the formation of Cs_2MoO_4 at temperatures below 500°C in the gap between fuel and clad [21].

It is of interest to estimate the oxygen distribution in a hyperstoichiometric mixed oxide fuel in which the O/(U + Pu) ratio is arrested by the buffering function of molybdenum. For this reason the thermodynamic equilibrium between MoO_2 and $(U_{0.8}Pu_{0.2})O_{2+x}$ has been estimated as a function of temperature using thermodynamic data which were taken from [17,18]. The obtained values of x for which thermodynamic equilibrium exists are plotted against the relative radius taking into account the temperature distribution of the RAPSODIE monitor experiment [20]. This values of x lie on the full line in fig. 6. The dotted line with an overall O/(U + Pu) = 4.008 represents the oxygen distribution which establishes during the oxydation of molybdenum. If molybdenum is fully oxidized, a further increase of the oxygen profile can occur as shown by the dashed line representing an overall O/(U + Pu) ratio of 4.013.

On the basis of the above considerations a practical example has been constructed and represented in fig. 7. As a starting material for a fast reactor fuel pin $(U_{0.8}Pu_{0.2})O_{2-y}$ with $0.2 < y < 0.3$ was chosen. This range of y represents a compromise between the need for a low O/(U + Pu) ratio and its industrial feasibility. Low O/(U + Pu) ratios diminish uranium-plutonium redistribution and the attack on the cladding [20,22]. Post irradiation examinations showed that after 7%

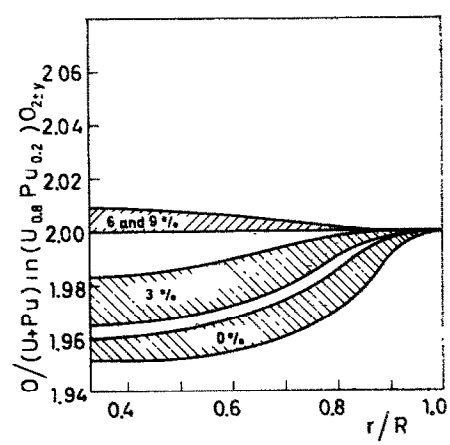

Fig. 7. Calculated radial oxygen distribution in a mixed oxide fuel, $(U_{0.8}Pu_{0.2})O_{2\pm y}$, with an initial O/(U + Pu) ratio between 1.97 and 1.98. Parameter is the burnup.

burnup a high and low attack on the cladding exists by a mixed oxide fuel with an O/M ratio higher and lower than 1.98, respectively [23]. This critical O/M value is independent of the concentration of plutonium in the mixed oxide [20].

Oxygen profiles have been calculated for burnups of 0, 3, 6 and 9% fima. The results are depicted in three zones each of them representing the consequence of the variation of the initial y. After 3% fima the fuel is still hypostoichiometric and the oxygen profile lies within the shaded area. Between 4 and 6% fima the total O/(U + Pu) nears 2 as it is shown in fig. 5. Between 6 to 9% fima the oxygen profile approaches the upper limit of the hyperstoichiometric zone which is governed by the buffering action of molybdenum.

From the standpoint of compatibility problems, an interesting point to consider is the variation of the oxygen concentration at the rim of the fuel. Fig. 8 represents the variation of y at the rim of the fuel as a function of burnup for the y range considered in fig. 7. For the chosen y range a steep increase in oxygen potential appears between a burnup of 4 and 6% fima. This increase is arrested by the buffering function of molybdenum. For burnups higher than 10% fima the molybdenum becomes fully oxydized and a further increase of the oxygen potential occurs.

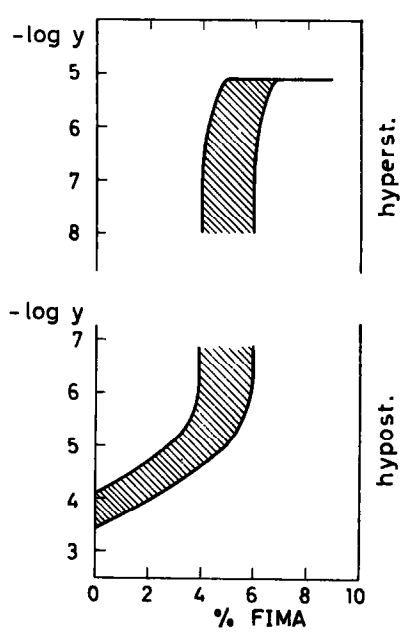

Fig. 8. Calculated variation of y at therim of mixed oxide fuel $(U_{0.8}Pu_{0.2})O_{2\pm y}$ for initial O/(U + Pu) ratios between 1.97 and 1.98 as a function of burnup.

7. Conclusion

The oxygen transport by way of vacancies and interstitials was investigated in hypo- and hyperstoichiometric uranium-plutonium mixed oxides, respectively. The results show that the heat of transport depends on the uranium and plutonium valence. The obtained values allow a calculation of oxygen profiles in reactor fuel pins.

It was shown that the heat of solid state transport consists of two terms. One represents the activated atomic jump processes, the other the movement of ions in a thermoelectric field. For a hypostoichiometric oxide, a comparison of the results obtained in axial and radial experiments reveals that thermoelectric forces make a minor contribution to the effective heat of transport. In hyperstoichiometric fuel the lattice energies have a minor influence on solid state transport; thermoelectric forces are predominant. This explains the migration of oxygen towards high temperatures. It should be noted that, despite the fact that the value of the thermoelectric power is not known, the experimental values of the effective heat of transport are suitable for describing the oxygen behavior in fuel pins.

The oxygen transport processes cause a small oxygen variation at the rim of the fuel also with a significant change of the total O/M. Nevertheless, this small O/(U + Pu) increase with burnup corresponds to a large increase of oxygen potential from which cladding corrosion problems arise. Such problems begin in a fuel with initial O/(U + Pu) = 1.97 after 6% burnup and with 1.98 after 4% burnup. Mixed oxide fuel with O/(U + Pu) not higher than 1.98 should be used in fast reactor pins, since it is advantageous to postpone the beginning of corrosion as far as possible.

References

[1] M.H. Rand and L.E.J. Roberts, Thermodynamics, Proc. IAEA Symp., Vienna 1966, Vol. I, p. 3.

[2] M.H. Rand and T.L. Markin, Thermodynamics of Nuclear Materials, 1967, Proc. IAEA Symp., Vienna 1968, p. 637.
[3] S.K. Evans. E.A. Aitken and C.N. Craig, J. Nucl. Mater. 30 (1969) 57.
[4] F.A. Aitken, J. Nucl. Mater. 30 (1969) 62.
[5] M. Bober, C. Sari and G. Schumacher, J. Nucl. Mater. 39 (1971) 265.
[6] M.G. Adamson, E.A. Aitken, S.K. Evans and J.H. Davies, Thermodynamics of Nuclear Materials 1974, Proc. IAEA Symp., Vienna 1975, p. 39.
[7] C. Sari and G. Schumacher, Thermodynamics of Nuclear Materials 1974, Proc. IAEA Symp., Vienna 1975, p. 73.
[8] C. Sari and G. Schumacher, J. Nucl. Technol., in print.
[9] F. Quick and C. Sari, J. Nucl. Mater. 47 (1973) 219.
[10] S.R. De Groot, Thermodynamics of irreversible processes (North-Holland Publ. Co., Amsterdam 1951).
[11] A.B. Lidiard, Thermodynamics, Proc. IAEA Symp.. Vienna 1966, Vol. II, p. 3.
[12] M. Bober and G. Schumacher, Material transport in the temperature gradient of fast reactor fuels, Ch. 2, Advances in Nuclear Science and Technology Vol. 7 (Academic Press, New York 1973).
[13] M. Bober, S. Dorner and G. Schumacher. Fuel and fuel elements for fast reactors, Brussels 1973, Proc. IAEA Symp., Vienna 1974, p. 221.
[14] P. Chereau and J.F. Wadier, J. Nucl. Mater. 46 (1973) 1
[15] K. Wirtz, Physik.Z. 44 (1943) 221.
[16] M.G. Adamson and R.F.A. Carney, J. Nucl. Mater. 54 (1974) 121.
[17] W. Breitung, GfK Report KFK 2091 (1975).
[18] O. Kubaschewski, E.L. Evans and C.B. Alcock. Metallurgical Thermochemistry (Pergamon Press 1967).
[19] M. Bober, H. Kleykamp and G. Schumacher, Nucl. Technol. 26 (1975) 172.
[20] M. Bober and G. Schumacher. GfK Report KFK 1965 (1975).
[21] H. Kleykamp, Reaktortagung Berlin 1974, p. 253.
[22] O. Götzmann, P. Hofmann and F. Thümmler, J. Nucl. Mater. 52 (1974) 33.
[23] W. Dienst, O. Götzmann, G. Ondracek and H. Zimmermann, in GfK Report KFK 1273/1 (1973) 112–14.